

Distribution dynamics of perfluorocarbon delivery to the lungs: an intact rabbit model

J. L. Bull,¹ S. Tredici,² E. Komori,² D. O. Brant,² J. B. Grotberg,¹ and R. B. Hirschl²

¹Biomedical Engineering Department and ²Department of Surgery, The University of Michigan, Ann Arbor, Michigan 48109

Submitted 28 October 2003; accepted in final form 14 December 2003

Bull, J. L., S. Tredici, E. Komori, D. O. Brant, J. B. Grotberg, and R. B. Hirschl. Distribution dynamics of perfluorocarbon delivery to the lungs: an intact rabbit model. *J Appl Physiol* 96: 1633–1642, 2004. First published December 19, 2003; 10.1152/jappphysiol.01158.2003.—Motivated by the goal of understanding how to most homogeneously fill the lungs with perfluorocarbon for liquid ventilation, we investigate the transport of liquid instilled into the lungs using an intact rabbit model. Perfluorocarbon is instilled into the trachea of the ventilated animal. Radiographic images of the perfluorocarbon distribution are obtained at a rate of 30 frames/s during the filling process. Image analysis is used to quantify the liquid distribution (center of mass, spatial standard deviation, skewness, kurtosis, and indicators of homogeneity) as time progresses. We compare the distribution dynamics in supine animals to those in upright animals for three constant infusion rates of perfluorocarbon: 15, 40, and 60 ml/min. It is found that formation of liquid plugs in large airways, which is affected by posture and infusion rate, can result in a more homogeneous liquid distribution than gravity drainage alone. The supine posture resulted in more homogeneous filling of the lungs than did upright posture, in which the lungs tend to fill in the inferior regions first. Faster instillation of perfluorocarbon results in liquid plugs forming in large airways and, consequently, more uniform distribution of perfluorocarbon than slower instillation rates in the upright animals.

liquid ventilation; surfactant replacement therapy; liquid bolus

DIRECT INSTILLATION OF A LIQUID bolus into the lungs is common to a number of pulmonary events and clinical treatments. For example, the delivery of exogenous surfactants into the lungs, surfactant replacement therapy (SRT) (18), is a common treatment for neonates with respiratory distress syndrome (RDS). The motivation of this study is the instillation of perfluorocarbon (PFC) liquid into the lungs for liquid ventilation. Liquid ventilation involves filling the lungs with PFC liquid and ventilating with either a gas [in partial liquid ventilation (PLV)] or liquid [in total liquid ventilation (TLV)] (5, 15, 16, 33–35). In PLV, it is desirable to form a liquid film that coats the airways and alveoli at end inspiration. In TLV, the lungs are completely filled with PFC and it is desirable to avoid gas trapping and overinflation of the lungs.

If liquid is instilled in a large enough quantity and given over a short enough period of time, it can occlude airways to form liquid plugs (7). These plugs can become air blown during inspiration, or they may drain because of gravity, or both. The liquid plug phenomenon is likely operative in the trachea and larger airways. Important aspects of the flow are the plug

velocity and the thickness of the trailing film left behind as functions of the driving pressure and fluid and tube physical properties. Typically the liquid plug ruptures and then transport is dominated by gravity drainage. The liquid layer thins to a monolayer in the small airways and surface tension gradients drive the flow of the liquid there (7, 13). Spreading of monolayers has been examined theoretically and experimentally both by our group and by others (1, 2, 8, 10).

Previous studies have investigated the instillation of liquids into animal lungs. Most of these studies have considered only the final distribution of the instilled liquid, usually surfactant (27, 38). Typically, a radiolabeled surfactant is mixed with dye-labeled microspheres and instilled into the lungs. The lungs are then flash frozen and cut into many (50 to 120) slices. The effects of surfactant type (11), dose size and number (38), instillation technique (27, 32, 38), and ventilation type (29, 30) on final distribution have been studied in this manner. However, little work has considered the dynamics of how the liquid reaches the final destination. An exception to this is our previous work on SRT (4), which considered surfactant mixed with a radiopaque marker instilled into excised rat lungs. In that paper, the surfactant was instilled such that it either drained down the sides of the trachea or formed a liquid plug in the trachea. The dose size in SRT (18, 22) is much smaller than in liquid ventilation, 2–5 ml/kg body wt compared with 20–40 ml/kg. The goal of the present work is to study the distribution dynamics when a higher volume of liquid is instilled, including the effects of instillation rate and posture.

PFCs have low surface tension and high oxygen and carbon dioxide solubilities and have been shown to improve lung mechanics and gas exchange in animal models of lung injury (9, 14, 16, 17, 33–36). Previous work has focused on the mechanisms by which gas exchange is improved by PLV (6, 11, 14, 16, 17, 19–21, 25). Functional residual capacity and pulmonary compliance are increased (17, 39), and pulmonary blood flow is redistributed to the better aerated regions of the lung (9, 36). Randomized, controlled pilot studies have suggested improvement in gas exchange during PLV compared with conventional ventilation in patients <55 yr of age with the acute RDS or acute lung injury (14) and a significant reduction in progression to acute RDS in patients with PLV (15). However, no significant difference in ventilator-free days was noted for patients with PLV compared with those with conventional mechanical ventilation (15). Despite potential benefits of PLV, further evaluation of beneficial effects and safety issues related to its

Address for reprint requests and other correspondence: J. L. Bull, Dept. of Biomedical Engineering, The Univ. of Michigan, 1107 Gerstacker Bldg., 2200 Bonisteel Blvd., Ann Arbor, MI 48109 (E-mail: joebull@umich.edu).

The costs of publication of this article were defrayed in part by the payment of page charges. The article must therefore be hereby marked “advertisement” in accordance with 18 U.S.C. Section 1734 solely to indicate this fact.

clinical use is needed (15, 23, 24). Other work has focused on expiration in TLV, in which a liquid tidal volume is used, and on how to avoid flow limitation or "choked flow" because of airway collapse (26). However, there has been little previous work on how to most homogeneously to fill a lung for liquid ventilation. In this paper, we specifically investigate the effects of patient posture and PFC instillation rate on the dynamics of PFC distribution using an intact, live rabbit model.

MATERIALS AND METHODS

Experiments. This experimental protocol was reviewed and approved by the University Committee on Use and Care of Animals. New Zealand White rabbits were weighed and anesthetized with intramuscular xylazine (5 mg/kg) and ketamine (20 mg/kg). After sedation, an intravenous catheter was placed in the ear and heparin was administered (1,000 units/kg). A tracheotomy was performed, and a steel endotracheal tube, 3/16-in. diameter and 3-cm length, was inserted 1.5–2.0 cm into the trachea. The endotracheal tube was doubly secured with silk suture. The endotracheal tube was connected to a 2-cm section of Tygon tubing which connected to a Y fitting. Tygon tubing connected the Y to a small animal ventilator (Harvard Apparatus, Holliston, MA). Pancuronium (0.1 mg/kg) was administered intravenously. The rabbit was then mechanically ventilated with a tidal volume of 24 ml, a frequency of 40/min, and an inspiratory-to-expiratory ratio of 1:1. The tidal volume was ~8 ml/kg for each rabbit, as the body weight of each animal was ~3.0 kg, e.g., 3.0 ± 0.1 kg. We used the same tidal volume and frequency for each rabbit, to have the same gas velocity within the endotracheal tube for each experiment. The gas flow within the endotracheal tube likely has an effect on the velocity of liquid plugs formed in large airways, and we wished to minimize variations of this between animals. A series of images of the lung during ventilation, but before PFC instillation, was also recorded and used for subtraction. X-ray images were acquired at 30 frames/s before and during PFC instillation by a high-resolution fluoroscopy unit (Philips portable c-arm, Philips Medical Systems, Amsterdam, The Netherlands), which is housed at The University of Michigan Medical Center and recorded on a digital video tape recorder (DCR-TRV 310 NTSC, Sony, Tokyo, Japan).

After the liquid-free images were acquired, PFC was continuously instilled into the endotracheal tube through a 23-gauge needle (inserted through the wall of the 2-cm section of Tygon tubing, with the hole sealed by tape) connected to a syringe pump (Sage Instruments, Freedom, CA). The rabbit was positioned either supine or upright (suspended with its spine vertical, its head at top and rear feet at bottom), and PFC was instilled at a rate of 15, 40, or 60 ml/min. These values were chosen to provide a range of filling rates, without filling so fast that most of the PFC refluxes into the Tygon tubing connecting the endotracheal tube to the ventilator. In clinical trials of PLV (14), the PFC is typically delivered slowly through a side port in the ventilator connect, such that there is minimal liquid reflux. The experiments presented here were designed to mimic the clinical setting. The maximum flow rate was chosen to be slow enough that liquid reflux was not appreciable at the start of instillation (60 ml/min). The other two rates were chosen to provide rates that were considerably slower but still possible with our experimental setup.

In PLV, the lungs are usually filled with liquid to functional residual capacity. Estimating functional residual capacity to be between 15 and 20 ml/kg, we used a total instillation volume of 60 ml. We did not base the instilled volume on weight because we wanted each animal to have the same time of instillation and same Reynolds numbers (ratio of inertial and viscous forces) of the instilled liquid at a given instillation rate. Animals of ~3.0 kg (3.0 ± 0.1 kg, ranging from 2.9–3.1) were selected for the

experiments to eliminate any effect that body weight variances might introduce. The experiments model lung filling in PLV and approximately the first half of lung filling in TLV. After the completion of the experiment, the rabbit was euthanized with an intravenous injection of Beuthanasia (Schering-Plough Animal Health, Union, NJ) (0.5 ml/kg). A necropsy was performed on each animal to assess the presence of PFC in the pleural spaces (per-fluorothorax), and, if PFC was identified, the animal was not included in data analysis. These experiments were conducted with seven animals for each posture-instillation rate combination. The data analysis was conducted for each animal and the results then averaged for all animals in the same posture-instillation rate combination. The results are presented as means \pm SE.

Analysis. The X-ray videos of the PFC instilled into the lungs were viewed, and qualitative observations were made regarding the homogeneity of distribution and the presence (or absence) of liquid plugs in airways. To quantify the homogeneity and other indicators of the liquid distribution, we used image-analysis techniques as follows. The digital video was captured to a dual processor, Intel Pentium III-based computer (Precision Workstation 220, Dell, Round Rock, TX) via an IEEE1394 card (DV Raptor, Canopus, San Jose, CA). The video was converted to a sequence of numbered bitmap images by use of Adobe Premier (Adobe Systems, San Jose, CA). These raw grayscale 640- by 480-pixel bitmap images were then loaded in Matlab (Mathworks, Natick, MA) as a double precision matrix in which each entry corresponds to the intensity, $I^*(x, y)$, of an individual pixel. In these two-dimensional images, $I^*(x, y)$ ranges from 0 (black) to 255 (white). These images were then rescaled so that $I = 255 \times [\text{ones matrix}] - I^*$, where I ranges from 0 (white) to 255 (black) and [ones matrix] is a matrix in which every entry has the value 1. The matrix $J(x, y)$ representing a preinstillation image at the same time in the breathing cycle was digitally subtracted (by using Beer's law) from each of the images during the liquid instillation so that only the radiopaque shadow remained visible.

The image without liquid for subtraction was calculated within the image analysis program, on the basis of the time in the breathing cycle and the breathing frequency indicated on the ventilator. Five frames before and after the calculated image were also evaluated to account for slight errors in the ventilator settings. Each image without liquid was subtracted from the image with liquid and the number of negative pixels determined. Negative intensity values of the subtracted (with liquid – without liquid) image indicated the lung tissue did not line up in the two images. If the lung tissue was perfectly aligned in the two images, every pixel would have a positive intensity value because only the liquid would remain. The image without liquid for subtraction was selected such that the number of negative pixels was minimized. Accurate selection of the image without liquid for the subtraction process was essential to the image analysis, because the appearance of the chest wall and ribs in the subtracted image could cause errors in the analysis.

Beer's law (37) relates the illumination of the radiopaque material in an X-ray to the path length through the radiopaque material, z , via

$$I(x, y, t) = I_0(x, y, t)e^{-mz} \quad (1)$$

where I is the intensity of an image containing material, I_0 is the intensity of an image without material, and m is the absorption coefficient of the material. If tissue without liquid is considered, the equation becomes

$$I_T(x, y, t) = I_{FF}(x, y, t)e^{-m_T z_T} \quad (2)$$

where I_T is the intensity of the tissue image, I_{FF} is the intensity of the flood field (light source) without the tissue, m_T is the adsorption coefficient of the tissue, and z_T is the path length through the tissue. For an image containing tissue in which the liquid is of interest, the equation becomes

$$I_L(x, y, t) = I_T(x, y, t)e^{-m_L z_L} \quad (3)$$

where I_L is the intensity of the liquid, m_L is the adsorption coefficient of the liquid, and z_L is the path length through the liquid. The scaled intensity matrix is determined by substituting Eq. 2 into Eq. 3 and using element-by-element math to determine $m_L z_L$

$$\hat{I}(x, y, t) = m_L z_L(x, y, t) = -\log \left[\frac{I_L(x, y, t)}{I_T(x, y, \tau)} \right] \quad (4)$$

where τ is the time during the cycle, $t = \tau + T \times n$ is time, T is the period of the breathing cycle, and n is the breath number. We use a single cycle of the lungs ventilated without liquid to determine I_T . The matrix \hat{I} was then filtered by using a thresholding process to minimize digital noise. A blocking window was then used to crop the image to consider only the section of the image that contained the lungs, by setting the intensity everywhere else equal to zero.

A statistical analysis was then performed on \hat{I} to assess the spatial distribution of PFC. The distribution of liquid mass within the image is characterized by a probability density function, $P(x_0, y_0)$, where x_0 and y_0 are dummy variables in the x and y directions, respectively

$$P(x_0, y_0) = \frac{\hat{I}(x_0, y_0)}{\int_{-\infty}^{\infty} \int_{-\infty}^{\infty} \hat{I}(x, y) dx dy} \quad (5)$$

Note that we have dropped the t from the intensity and let it be implied that we are considering a single image corresponding to a specific time. In both the supine and upright images, we consider x to lie along the direction of the trachea and y to be normal to the x direction.

The x -direction statistics are determined by first finding the moments about the x mean (\bar{x})

$$M_k(y) = \int_{-\infty}^{\infty} (x - \bar{x})^k P(x, y) dx \quad (6)$$

The average value for the k th moment is

$$M_k = \int_{-\infty}^{\infty} M_k(y) dy = \int_{-\infty}^{\infty} (x - \bar{x})^k g(x) dx \cong \sum_{x=1}^m (x - \bar{x})^k g(x) \quad (7)$$

where the marginal probability density function is defined as

$$g(x_0) = \frac{\int_{-\infty}^{\infty} \hat{I}(x_0, y) dy}{\int_{-\infty}^{\infty} \int_{-\infty}^{\infty} \hat{I}(x, y) dx dy} \cong \frac{\sum_{y=1}^n \hat{I}(x_0, y)}{\sum_{x=1}^m \sum_{y=1}^n \hat{I}(x, y)} \quad (8)$$

and m and n are the dimensions of the matrix \hat{I} in the x and y directions, respectively. Figure 1 shows an image of the lung partially filled with PFC. Computing the x -direction statistics is analogous to dividing the image into slices (a sample slice is shown), lumping the mass of the slice at its x value, and then computing one-dimensional statistics based on these lumped masses. This is illustrated by the graph of $g(x_0)$ in Fig. 1. The slice shown in the lung image corresponds to the slice shown on the graph, and slices from the entire image result in the graph shown. The following statistical quantities are defined in terms of the first four moments: mean value or center of mass is given by $\bar{x} = M_1$ when Eq. 4 is calculated with respect to the global coordinate system rather than the center of mass; spatial standard deviation, $\sigma_x = (M_2 - M_1^2)^{1/2}$; skewness, $skew_x = M_3/\sigma_x^3$; and kurtosis, $kurt_x = M_4/\sigma_x^4 - 3$. The corresponding horizontal statistics may be computed by using Eqs. 2-5 in the y direction. Skewness is an indicator of the distribution around the mean. A

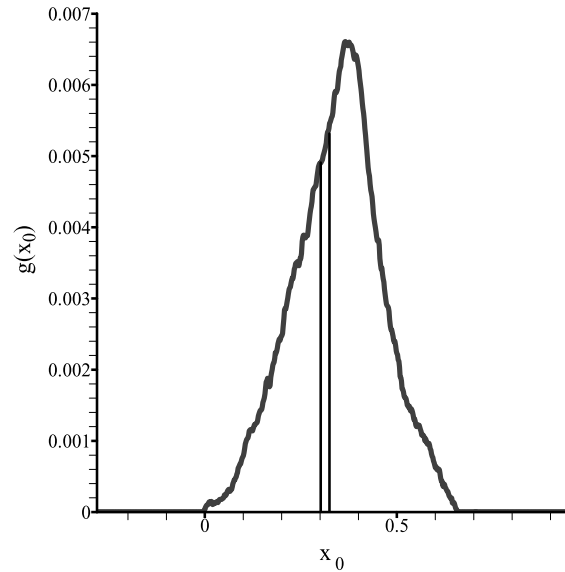
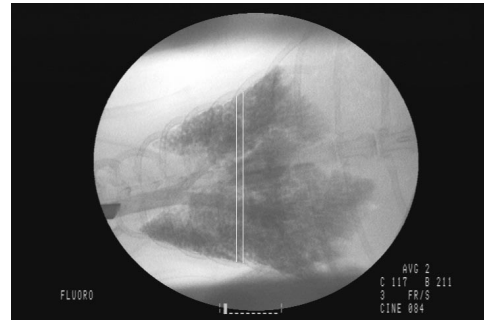


Fig. 1. Image of lungs that are partially filled with liquid and corresponding graph of $g(x_0)$, which is used in calculation of statistics in the x direction. The calculation of $g(x_0)$ involves subtracting the lung image without liquid from the image with liquid (using Beer's law) and sectioning the resulting image into slices that lie in the y direction. The mass in each slice is then added up to produce $g(x_0)$. This is then used to calculate the x -direction statistics. An analogous approach is used for the y -direction statistics.

positive (negative) skewness indicates an asymmetric tail extending in the positive (negative) x direction. Kurtosis indicates the peakedness or flatness of a distribution relative to a normal distribution. A positive (negative) kurtosis indicates the distribution is more peaked (flat) than a normal distribution (3, 31).

To assess the distribution of liquid, the lung images were sectioned into quadrants and the fraction of each quadrant reached by PFC was calculated. The centerline of the lungs, along the trachea, and a line halfway between the superior and inferior edges of the lungs defined the quadrants of the lung image. If a pixel had an \hat{I} above a threshold value, $\hat{I} = 0.2 \times \hat{I}_{max}$, it was considered to have been reached by the PFC. The number of pixels reached by PFC was calculated for each quadrant, and the fraction of each quadrant reached by PFC was determined by dividing its number of pixels reached by the total number of pixels in the quadrant. The homogeneity of the distribution in the lungs was indicated by a homogeneity index, HI, that was calculated as the ratio of the highest fraction reached to the lowest fraction reached. Thus the HI is between 0 and 1 and is a gross-scale indicator of how homogenous the lungs are filled.

We compared the experimental statistics (center of mass, spatial standard deviation, skewness, and kurtosis) to corresponding statistics from a theoretical model of a single liquid plug that is blown through a single straight tube. Halpern et al. (13) approximated liquid plug

motion by a semi-infinite bubble in a tube and determined the dimensionless trailing film thickness, $f = h/a$, of a steadily moving bubble as a function of capillary number, Ca . Note that a is the tube radius, and capillary number, $Ca = \mu U/\sigma$, is the ratio of viscous force to surface tension force. Fluid viscosity and surface tension denoted by μ and σ , respectively, and U is the speed of the liquid plug. Halpern et al. estimate

$$f(Ca) = 0.36[1 - e^{-2Ca^{0.523}}] \quad (9)$$

From conservation of mass, the volume density of the liquid $\rho(x)$ is approximately

$$\rho(x) = \begin{cases} 2\pi a^2 f, & 0 \leq x \leq x_T \\ \pi a^2, & x_T \leq x \leq x_T + L \end{cases} \quad (10)$$

where x_T is the location of the rear meniscus of the plug and L is the plug length. Integrating the volume and scaling time, t , so that $T = t/T_f$, where T_f is the time at which the plug ruptures, we can obtain the dimensionless k th moment of the distribution to be

$$\begin{aligned} \hat{M}_k(T, Ca) &= \frac{M_k}{\pi a^2 L_0^{k+1}} \\ &= \frac{1}{k+1} \left\{ \left(\frac{T}{2f} \right)^{k+1} (2f-1) + \left[\frac{T}{2f} (1-2f) + 1 \right]^{k+1} \right\} \quad (11) \end{aligned}$$

for $0 \leq T \leq 1$. Statistics for this theoretical distribution of liquid from a single liquid plug moving at constant speed in a single tube were calculated by using these moments. Typical liquid plug velocities from the video were ~ 3 cm/s, resulting in $Ca \sim 4 \times 10^{-3}$. This value of Ca was used to calculate $f(Ca)$.

RESULTS

A total of 42 animals (7 at each instillation rate-posture combination, 3.0 ± 0.1 kg) were used, and none was found to have perfluorothorax. After the analysis of data from each animal, the results of these experiments were nondimensionalized, with length scaled by lung length and time scaled by time of PFC instillation. By this scaling, nondimensional time can alternatively be thought of as the fraction of total liquid instilled. This dimensionless data for all animals at a given posture-instillation rate were averaged to produce a mean \pm standard error at that condition. Figure 2 shows images of lungs during the filling process in both postures, and Figs. 3–6 show the quantitative data corresponding to observed behavior.

Figure 2 shows the liquid distribution at dimensionless times of 0, 0.25, and 0.5 (i.e., when no PFC had been instilled, one-quarter of the PFC instilled, and one-half of the PFC instilled) for supine and upright animals with an instillation rate of 60 ml/min. In the supine posture (Fig. 2, A–C), the distribution appears fairly uniform as time progresses, with the liquid-filled regions becoming darker (i.e., more liquid mass) as the lungs become more filled. In the upright posture (Fig. 2, D–F), the lungs fill from the inferior regions upward. As time progresses, the PFC level rises, with little liquid reaching the superior lobes of the lungs. We observed that liquid plugs formed in the trachea and large airways more frequently for the supine animals than for the upright animals at a given PFC instillation rate. When liquid plugs did form in the large airways of upright animals, gravity, in addition to the air-blown liquid plug dynamics, likely influenced their propagation, resulting in preferential filling of the inferior regions of the lungs in the upright posture. From images, it was apparent that liquid

plugs formed on each breath and were transported into the lungs until they ruptured. At that point transport was driven by gravity drainage and pressure gradients within the liquid layer. Liquid plugs were also observed to reform in large airways on expiration late during the instillation process. This was due to capillary instabilities of the PFC layer, which likely thickened as the lungs became fuller and sometimes led to PFC reflux out of the lungs.

Figure 3 contains plots of \bar{x} and σ_x vs. t (A) and of $skew_x$ and $kurt_x$ vs. t (B) for supine animals with an infusion rate of 60 ml/min. Each data point is the average of all (7) the animals at this condition. The values in A are scaled by lung length and the values in B are scaled by their respective maximum values. Figure 3 shows the resulting theoretical values of \bar{x} and σ_x vs. t (C) and $skew_x$ and $kurt_x$ vs. t (D). Spatial standard deviation, skewness, and kurtosis in the x and y directions do not appear strongly dependent on posture or instillation rate. Because these were not statistically different between the different cases, we only present these statistics for one parameter set (supine animal, instillation rate of 60 ml/min, skewness and kurtosis in x direction) here (Fig. 3B).

As shown in Fig. 3A, \bar{x} is initially near 0.2 because the lung is essentially void of PFC at time zero. When liquid is instilled, \bar{x} shifts to near the trachea, $x = 0$, and then propagates in the positive x direction as the lungs fill. The propagation of the center of mass is very dependent on the instillation rate and posture; these effects are shown in Fig. 4 and discussed below. From the theoretical model (Fig. 3C), the center of mass starts near $x = 0$ and then propagates along the tube until the plug ruptures. As shown in Fig. 3A, σ_x increases with time after an initial decrease for both the supine and upright animals. At $t = 0$, the spatial standard deviation in both directions is high relative to later times, indicating that the lungs are not filled with liquid and consequently the subtracted image is fairly uniform. When liquid enters the lungs, σ_x becomes small, indicating that the liquid mass is concentrated in a small area. As the lungs become more filled with liquid, σ_x increases. Similar behavior is observed in σ_y for both supine and upright posture (not shown). The theoretical σ_x starts near zero because the liquid plug is within the domain and then increases as the plug moves along the tube, leaving behind a thin film of liquid. The general behavior is similar to that observed in the experiments.

As indicated by the error bars in Fig. 3B, $skew_x$ varied greatly at early times between animals. The skewness started out near -1 and increased to approximately $+1$ in the first breath. As time progressed, $skew_x$ reached a slightly negative value. The small absolute value of $skew_x$ indicates a relatively symmetrical distribution about the mean. The negative value indicates that the asymmetry present in the distribution results in the tail toward negative values of x being larger. This is because the PFC is instilled in the trachea (smaller x) and propagates in the direction of increasing x . The skewness for the single-tube theoretical model starts out near zero and quickly increases before decreasing to near its initial value at later times, indicating that at later times this theoretical distribution is more symmetrical than at intermediate times. As shown in Fig. 3B, $kurt_x$ initially has a high variance and can be positive or negative, before approaching a nearly constant and slightly negative value at later times. Similar behavior is observed in $kurt_y$ (not shown). Near $t = 1$, the distribution is

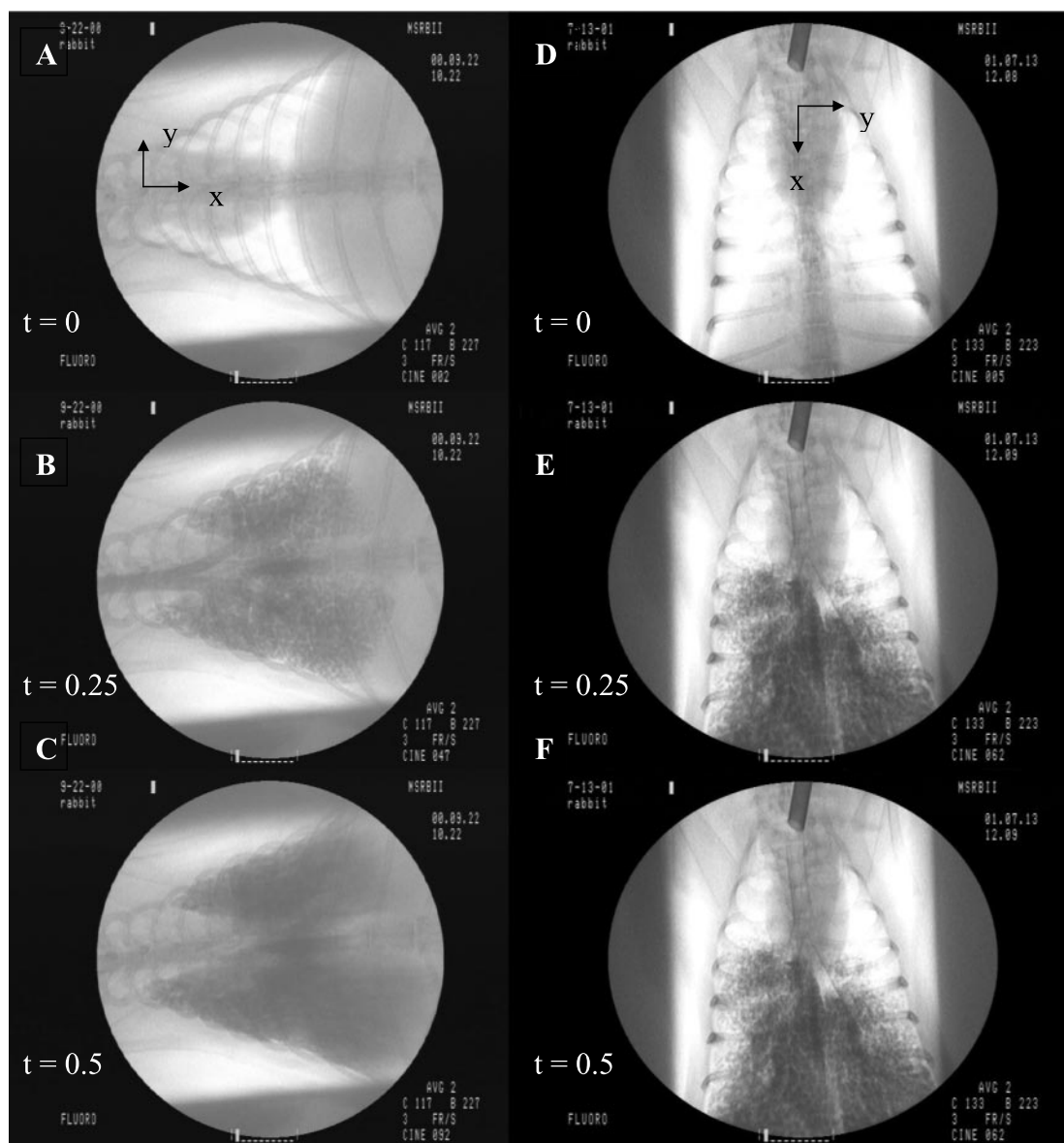


Fig. 2. Lung images for a supine animal with perfluorocarbon (PFC) instilled at a rate of 60 ml/min at dimensionless times $t = 0$ (A), $t = 0.25$ (B), and $t = 0.5$ (C) and lung images for an upright animal with PFC instilled at a rate of 60 ml/min at dimensionless times $t = 0$ (D), $t = 0.25$ (E), and $t = 0.5$ (F). Note that the PFC tends to fill the lungs of upright rabbits from the bottom up, whereas the supine lungs tend to fill more evenly. Time is nondimensionalized by total instillation time, so that $t = 1$ corresponds to the time at which all 60 ml of PFC has been instilled. Alternatively, dimensionless time can be thought of the fraction of total PFC that has been instilled.

flatter, i.e., more uniform, than a normal distribution, or platykurtic. The kurtosis in the single tube theoretical model, Fig. 3D, exhibits similar behavior.

Figure 4 shows plots of \bar{x} vs. t for supine and upright animals for each of the instillation rates, 15, 40, and 60 ml/min. As shown in Fig. 4, the \bar{x} center of mass propagates slower for the 15 ml/min instillation rate than for instillation rates of 40 and 60 ml/min for rabbits in the supine posture. When the animal is in the upright posture, the center of mass propagates slowest for the 60 ml/min instillation rate. The 15 and 40 ml/min instillation rates yield similar propagation rates at early times, but as time increases past 0.5 the \bar{x} center of mass moves in the negative direction for the 15 ml/min instillation rate. This behavior in the upright animal

is due to the formation of liquid plugs in the large airways at the fastest instillation rate. These plugs are then blown through the airway tree on inspiration. The slower instillation rates do not appear sufficient to form liquid plugs in the large airways, and transport is initially dominated by gravity drainage. Instillation rate, along with fluid properties and tube position, has been shown to affect the formation of liquid plugs in glass capillary tubes (7). When plugs are not formed in large airways, the liquid may pool in more distal airways to form plugs there. This behavior is likely responsible for the \bar{x} motion for 15 ml/min instillation rate. The liquid initially drains quickly, resulting in fast \bar{x} propagation. As more liquid is instilled, it pools to form plugs, which are then blown through the airways. The effect of

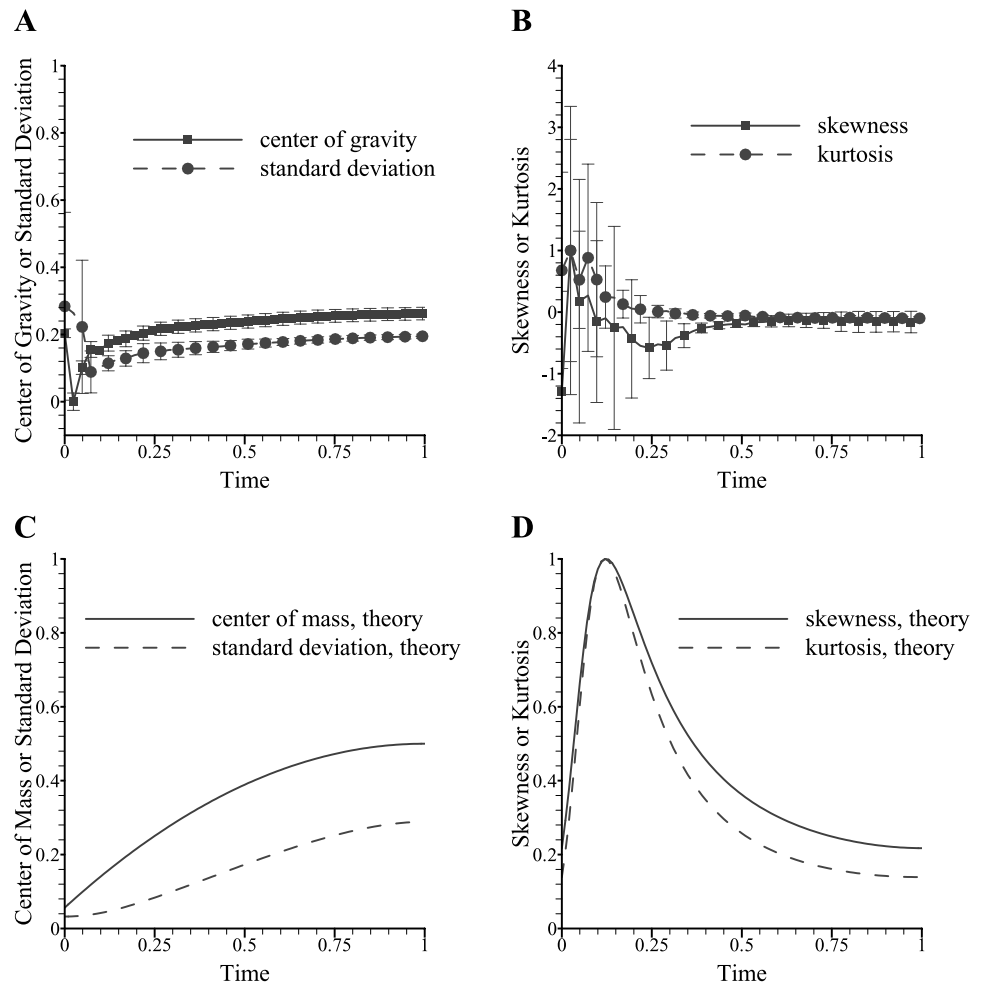


Fig. 3. Comparison of experimental statistics for supine animals (60 ml/min PFC instillation rate) and theoretical statistics for a semi-infinite bubble in a single tube: mean x (\bar{x}) and spatial standard deviation (σ_x) vs. t (A) and skewness ($skew_x$) and kurtosis ($kurt_x$) vs. t (B) for experiments; \bar{x} and σ_x vs. t (C) and $skew_x$ and $kurt_x$ vs. t (D) from theory.

gravity on liquid distribution is weaker when plugs are formed than it is when plugs are not formed. Plugs that occlude the airways are more readily blown along by ventilation than is a liquid film that air may flow past. The x center of mass does not propagate downward as quickly when plugs are formed because the plugs are transported more homogeneously through the airways.

Figure 5 shows fraction of lung quadrant reached ($I > 0.2$) vs. dimensionless time for supine animals with PFC instillation rates of 15 (A), 40 (B), and 60 ml/min (C), and for upright animals with PFC instillation rates of 15 (D), 40 (E), and 60 ml/min (F). The lung fraction reached by liquid for an instillation rate of 15 ml/min varies slightly with quadrant for the supine posture animal, as shown in Fig. 5A. Initially, the fraction reached for each quadrant is zero because there is no liquid in the lungs. As time progresses, the lungs fill with liquid and the fraction of each quadrant reached increases. For $t > 0.6$, the inferior quadrants have higher fractions reached than the superior quadrants. Despite these differences, the fraction reached for all quadrants is between 0.45 and 0.6 at $t = 1$ for the supine posture. When the animal is upright, the fraction reached depends strongly on the quadrant, as shown in Fig. 5D. Larger fractions of the inferior quadrants are reached than are reached in the superior quadrants. At $t = 1$, the fraction reached ranges from ~ 0.1 in the upper left quadrant to

nearly 0.8 in the lower right quadrant. Posture impacts the fraction reached for each quadrant significantly for the 15 ml/min instillation rate. Differences between the left and right superior or inferior quadrants appear to be due to lung morphometry and the asymmetry of the first airway bifurcation, with the less sharply angled branch being preferred. At low instillation rates, liquid plugs are likely not formed in the trachea for upright posture. Consequently, the distribution for this condition depends on gravity drainage and formation of liquid plugs in small airways and appears more strongly affected by bifurcation asymmetry than is the plug propagation in the supine animals.

Similar behavior is noted in comparing supine and upright animals at an instillation rate of 40 ml/min (Fig. 5, B and E). As for the supine animals with PFC instilled at a rate of 15 ml/min, the fraction reached does not exhibit as large differences between left and right lung quadrants for the supine animals as for the upright animals at 40 ml/min. At an instillation rate of 60 ml/min (Fig. 5C), the fraction reached for the lower quadrants is similar in the supine animals for all times. At later times, the two upper quadrants have similar fractions reached. The fraction reached varies between ~ 0.4 and 0.6 for an instillation rate of 60 ml/min in the supine animals at $t = 1$. The upright animals (Fig. 5F) have a noticeable difference between fractions reached of the upper and lower quadrants. However, at this instillation

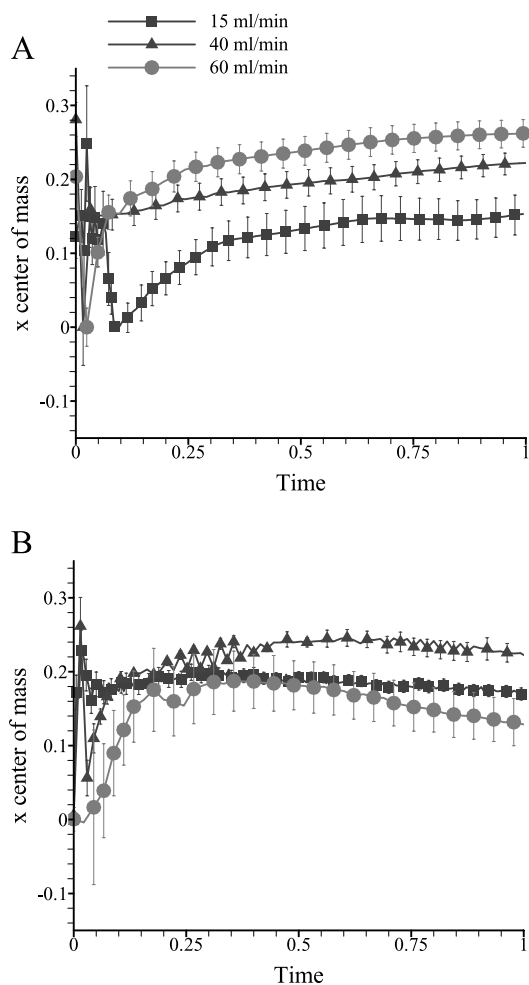


Fig. 4. Center of mass, \bar{x} , vs. time for supine (A) and upright animals (B) at instillation rates of 15 (■), 40 (▲), and 60 ml/min (●).

rate, lateral differences in fraction reached are small at each time. The difference between the fraction reached in the upper (~ 0.7) and lower (~ 0.4) quadrants is smaller for the 60 ml/min instillation rate than for the 40 and 15 ml/min instillation rates and is larger than in the supine animals at the same instillation rate. The faster instillation rate in the upright animal results in liquid plug formation in larger airways, including the trachea, (observed in X-ray images) and consequently results in closer agreement in fraction reached of upper and lower quadrants.

Figure 6 contains plots of HI (highest fraction reached in a quadrant divided by lowest fraction reached in a quadrant) vs. t for supine and upright animals, with PFC instillation rates of 15, 40, and 60 ml/min. HI vs. t depends on instillation rate and posture. Initially, HI is 1, because the lungs are empty and consequently homogenous. Soon after $t = 0$, liquid enters the lungs through the trachea and the distribution is no longer homogenous, and HI is low. As the lungs fill with liquid, HI increases. For the supine posture, instillation rates of 15 and 60 ml/min yield similar HI vs. t plots. HI for 40 ml/min is lower for $t > 0.5$. An instillation rate of 60 ml/min often formed plugs in large airways, whereas an instillation rate of 15 ml/min typically did not form liquid plugs in large airways. For 15 ml/min, the PFC must drain into small airways and pool to

form plugs there. The instillation rate of 40 ml/min appeared not to form liquid plugs in the trachea but often did past the first airway bifurcation. Gravity drainage dominated the transport before liquid plugs were formed, and the plugs did not appear to form at all airways at a given generation, leading to a less homogenous distribution than the other two instillation rates for the supine posture.

For upright posture, the 15 and 40 ml/min instillation rates have HI values ≤ 0.2 for all times. The 60 ml/min instillation rate has a higher HI compared with the slower instillation rates at all times and reaches HI ≈ 0.5 at $t = 1$. The formation of liquid plugs in larger airways with this instillation rate resulted in a more homogenous distribution of liquid. Despite this, the effects of gravity result in a less homogenous distribution than the same instillation rate in the supine posture, HI ≈ 0.5 compared with HI ≈ 0.7 . For the 15 ml/min instillation rate in the upright posture, the formation of liquid plugs was delayed until distal airways, as the liquid drained because of gravity in large airways and pooled in smaller ones to form liquid plugs. In the upright posture at this rate, airway bifurcation geometry seemed to strongly affect the distribution. At this instillation rate, plugs are less likely to form in the trachea and liquid pools to form plugs that are then blown into the lung regions distal to the location of plug formation. This results in the lateral differences in filling seen in Fig. 5 and the higher HI at 60 ml/min in Fig. 6.

DISCUSSION

The finding that liquid plug formation in large airways results in more homogeneous PFC distribution than when plugs do not form in large airways is similar to our previous findings in which varying the position of the instillation tube affected plug formation in the smaller doses of SRT in excised rat lungs (4). The plug formation in this work is affected by animal posture and instillation rate rather than instillation tube position. Liquid plugs tend to form more readily in the supine posture and consequently that posture results in more homogeneous filling. In the upright posture, the lungs tend to fill from the bottom upward. Instilling the PFC faster results in a greater tendency to form liquid plugs in the large airways, and the resulting air-blown plug flow produces a more homogeneous PFC distribution than gravity drainage alone. Plug formation remains important in the resulting homogeneity even as the volume of liquid in the lungs becomes large, as is the case in TLV or PLV. It appears from the propagation of individual plugs and the time evolution of the liquid distribution that instilled liquid at a given breath goes to similar locations as on the previous breath. This may change as the liquid lining thickens because of the film left behind by liquid plugs.

We also noted from the video that, on expiration, thick liquid linings reform plugs, which are then carried out of the lung (for dimensionless times near 1 and instillation rate of 60 ml/min). Thicker liquid linings are more prone to instabilities that result in airway closure (12). A strategy to prevent the reflux of instilled liquid in the clinical situation would be to instill liquid plugs slowly, so that they leave behind a thinner liquid layer. In the limit of $Ca \ll 1$, Eq. 9 yields $f \sim 0.72 Ca^{0.523}$, indicating a thinner trailing film for slower (smaller Ca) plug propagation.

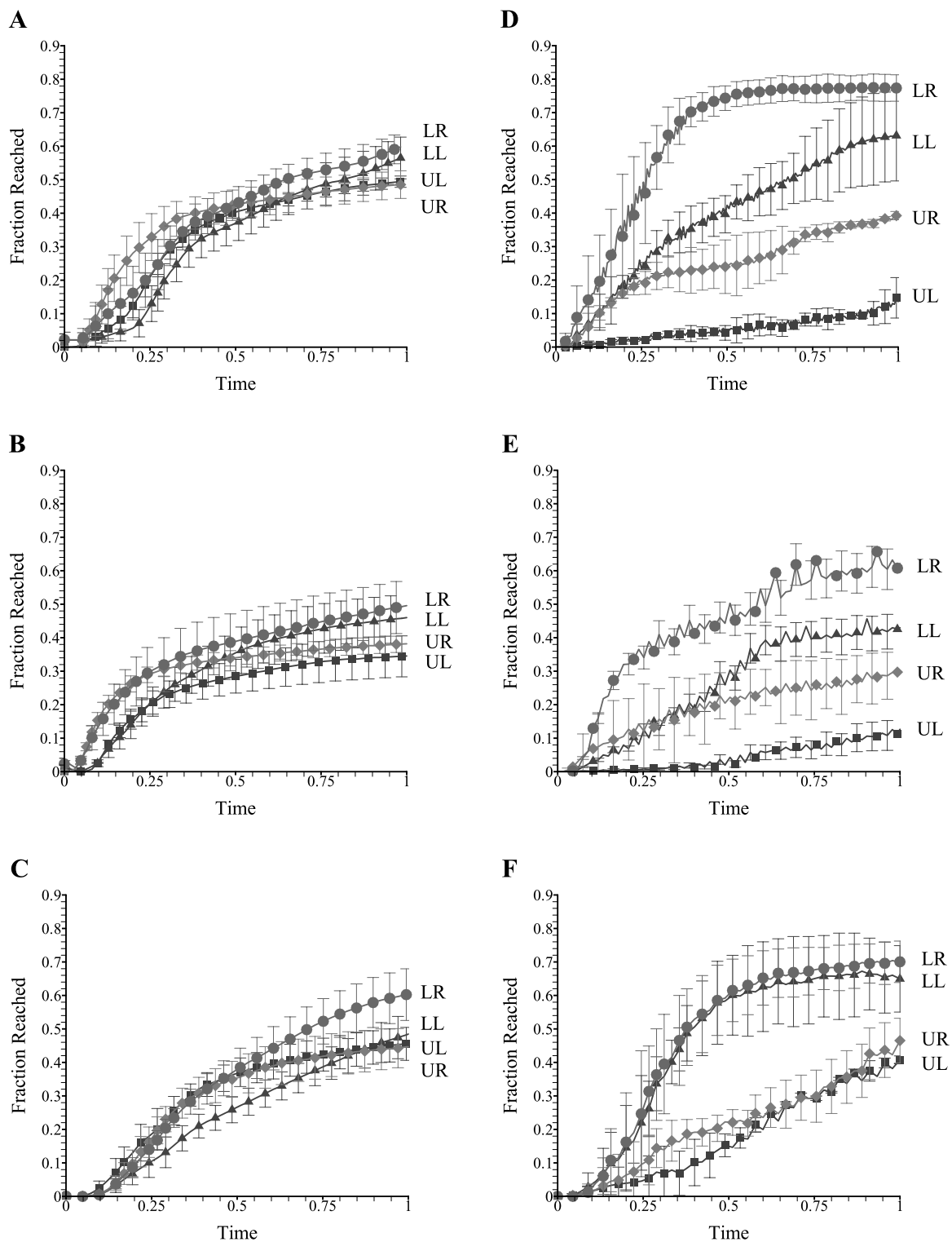


Fig. 5. Fraction reached vs. time for supine animals with instillation rates of 15 (A), 40 (B), and 60 ml/min (C) and fraction reached vs. time for rate upright animals with instillation rates of 15 (D), 40 (E), and 60 ml/min (F). The fraction reached is shown for each lung quadrant: upper left (UL, ■), lower left (LL, ▲), upper right (UR, ◆), and lower right (LR, ●). Note that the lungs of upright animals tend to fill in the inferior regions first and exhibit left-to-right asymmetry in filling. The fractions reached of each quadrant in the supine animals are more closely grouped.

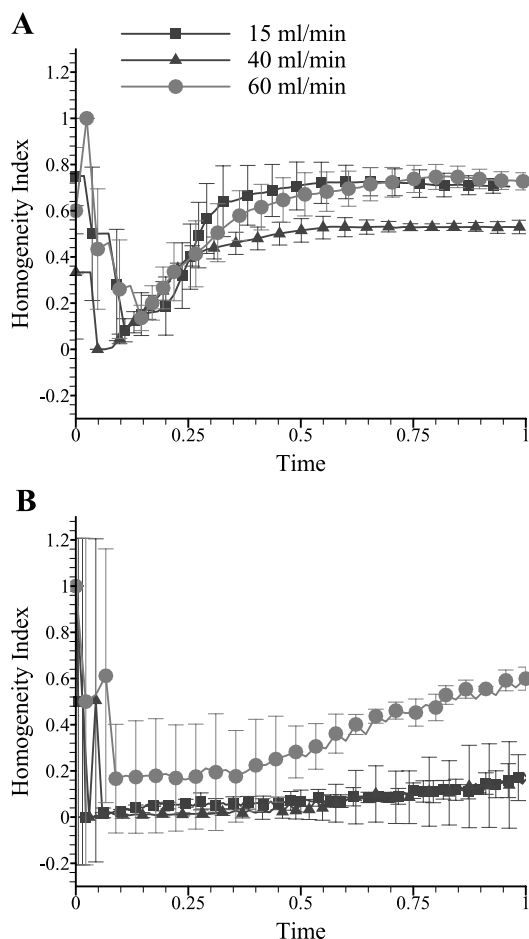


Fig. 6. Homogeneity index vs. t for supine (A) and upright animals (B), at instillation rates of 15 (■), 40 (▲), and 60 ml/min (●). In general, homogeneity index is higher for the supine animals than for the upright animals.

Although there has been little previous work on the distribution of instilled PFCs, previous studies have suggested that bolus instillation of surfactant results in a more homogeneous distribution than a constant infusion (32, 38). In these studies, the bolus instillation involved instilling a quarter dose of surfactant (typically 1 ml/kg) followed by 30 s of ventilation and then the administration of the remaining quarter doses at similar time increments until the entire dose was delivered. The constant infusion involved instilling the entire surfactant dose through a side port in the ventilator tubing over a period of 30 min. Both of these instillation techniques involved changing the position of the animal to allow gravity to act in a variety of directions. The constant infusion was found to result in a less homogeneous distribution than the bolus infusion method (32, 38). This is consistent with the present study, because we would expect liquid plugs to form in the bolus-instillation technique, and liquid plug formation in large airways is not very likely in the constant-infusion method because of the very slow infusion rate.

Despite this PFC delivery process being very complex and involving many liquid plugs rather than a single one, the single tube theoretical model captures some of the general trends of the distribution statistics. A more complicated theoretical model that accounts for multiple liquid plugs, the delivery of a

new plug with each breath, airway branching, and the potential for plug reformation would be more applicable to the results of this study. However, this simple analysis provides some indication of the distribution behavior that would be expected from an air-blown liquid plug, which shows some similarities to the experimental results due to the considerably more complicated effects of delivery of many liquid plugs.

A limitation of this study is that the two-dimensional imaging technique does not account for the distribution of liquid normal to the plane of the image. Using Beer's law accounts for the varying depth of PFC into the image but does not provide details of how it is distributed. It is expected that variations in this direction are less significant than variations in plane considered, particularly for the upright posture. To assess the importance of this, we imaged supine animals from a lateral view and were unable to observe variations in liquid distribution from the front to the back of the animal. This was in part due to the cardiac shadow blocking much of the lung image and the thinness of the lungs in that direction compared with the length from superior to inferior lobes. On the basis of this, we considered the two-dimensional images to provide adequate on the distribution of instilled liquid for comparison of upright and supine animals. However, a study that utilizes three-dimensional imaging could be a worthwhile future investigation. Although this investigation has considered the effects of several variables on distribution of instilled liquid for large instillation volumes, there are many other factors that are important. Future studies could investigate the effects of fluid properties, such as viscosity, density, and surface tension. Likewise, the effects of ventilation rate and tidal volume should also be addressed by future studies. This study has focused on the effects of instillation technique on the resulting PFC distribution. We expect the distribution to have an appreciable impact on the effectiveness of the pulmonary support provided by liquid ventilation, and these effects will be a topic for future studies.

In conclusion, our experimental results indicate that posture has a significant effect on distribution of instilled liquid, with upright posture resulting in lower homogeneity index and greater difficulty filling superior regions of the lung. Instillation speed influences resulting distribution. The fastest and slowest filling rates resulted in a more homogeneous distribution than the medium rate for supine animals. The faster filling resulted in a more homogeneous distribution for upright animals because it favored liquid plug formation in large airways. When liquid plugs are formed, either in large airways because of fast enough instillation or in distal airways because of pooling of liquid, the distribution distal to the location of plug formation is more homogeneous than if plugs had not formed. The effect of airway geometry on liquid plug transport does not appear as strong as the effect of airway geometry on gravity drainage without plug formation. The resulting distribution dynamics are important in delivering the instilled liquid to its desired location, and this may potentially allow specific regions of the lung to be targeted for delivery.

GRANTS

This research is funded by National Institutes of Health Grant HL-64373. J. L. Bull is a Parker B. Francis Fellow in Pulmonary Research.

REFERENCES

1. Bull JL and Grotberg JB. Surfactant spreading on thin viscous films: film thickness evolution and periodic wall stretch. *Exper Fluids* 34: 1–15, 2003.
2. Bull JL, Nelson LK, Walsh JT, Glucksberg MR, Schurch S, and Grotberg JB. Surfactant-spreading and surface-compression disturbance on a thin viscous film. *J Biomech Eng* 121: 89–98, 1999.
3. Cassella G and Berger RL. *Statistical Inference*. Pacific Grove, CA: Thomson Learning, 2002.
4. Cassidy KJ, Bull JL, Glucksberg MR, Dawson CA, Haworth ST, Hirschl RB, Gavriely N, and Grotberg JB. A rat lung model of instilled liquid transport in the pulmonary airways. *J Appl Physiol* 90: 1955–1967, 2001.
5. Clark LC Jr and Gollan F. Survival of mammals breathing organic liquids equilibrated with oxygen at atmospheric pressure. *Science* 152: 1755–1756, 1966.
6. Doctor A, Al-Khadra E, Tan P, Watson KF, Diesen DL, Workman LJ, Thompson JE, Rose CE, and Arnold JH. Extended high-frequency partial liquid ventilation in lung injury: gas exchange, injury quantification, and vapor loss. *J Appl Physiol* 95: 1248–1258, 2003.
7. Espinosa FF and Kamm RD. Meniscus formation during tracheal instillation of surfactant. *J Appl Physiol* 85: 266–272, 1998.
8. Espinosa FF, Shapiro AH, Fredberg JJ, and Kamm RD. Spreading of exogenous surfactant in an airway. *J Appl Physiol* 75: 2028–2039, 1993.
9. Gauger PG, Overbeck MC, Koeppe RA, Shulkin BL, Hrycko J, Weber ED, and Hirschl RB. Distribution of pulmonary blood flow and total lung water during partial liquid ventilation in acute lung injury. *Surgery* 122: 313–323, 1997.
10. Gaver DP and Grotberg JB. The dynamics of a localized surfactant on a thin film. *J Fluid Mech* 213: 127–148, 1990.
11. Greenspan JS, Fox WW, Rubenstein SD, Wolfson MR, Spinner SS, and Shaffer TH. Partial liquid ventilation in critically ill infants receiving extracorporeal life support. *Pediatrics* 99: E21–E25, 1997.
12. Halpern D and Grotberg JB. Fluid-elastic instabilities of liquid-lined flexible tubes. *J Fluid Mech* 244: 615–632, 1992.
13. Halpern D, Jensen OE, and Grotberg JB. A theoretical study of surfactant and liquid delivery into the lung. *J Appl Physiol* 85: 333–352, 1998.
14. Hirschl RB, Conrad S, Kaiser R, Zwischenberger JB, Bartlett RB, Booth F, and Cardenas V. Partial liquid ventilation in adult patients with ARDS: a multicenter phase I–II trial. *Ann Surg* 228: 692–700, 1998.
15. Hirschl RB, Croce M, Gore D, Wiedemann H, Davis K, Zwischenberger J, and Bartlett RH. Prospective, randomized, controlled pilot study of partial liquid ventilation in adult acute respiratory distress syndrome. *Am J Respir Crit Care Med* 165: 781–787, 2002.
16. Hirschl RB, Grover B, McCracken M, Wolfson MR, Shaffer TH, and Bartlett RH. Oxygen consumption and carbon dioxide production during liquid ventilation. *J Pediatr Surg* 28: 513–518, 1993.
17. Hirschl RB, Tooley R, Parent A, Johnson K, and Bartlett RH. Evaluation of gas exchange, pulmonary compliance, and lung injury during total and partial liquid ventilation in the acute respiratory distress syndrome. *Crit Care Med* 24: 1001–1008, 1996.
18. Jobe AH. Pulmonary surfactant therapy. *N Engl J Med* 328: 861–868, 1993.
19. Leach CL, Fuhrman BP, Morin FC, and Rath MG. Perfluorocarbon-associated gas exchange (partial liquid ventilation) in respiratory distress syndrome: a prospective, randomized, controlled study. *Crit Care Med* 21: 1270–1278, 1993.
20. Leach CL, Greenspan JS, Rubenstein SD, Shaffer TH, Wolfson MR, Jackson JC, DeLemos R, and Fuhrman BP. Partial liquid ventilation with perflubron in premature infants with severe respiratory distress syndrome. *N Engl J Med* 335: 761–767, 1996.
21. Leach CL, Holm B, Morin FC, Fuhrman BP, Papo MC, Steinhorn D, and Hernan LJ. Partial liquid ventilation in premature lambs with respiratory distress syndrome: efficacy and compatibility with exogenous surfactant. *J Pediatr* 126: 412–420, 1995.
22. Lewis JF and Jobe AH. Surfactant and the adult respiratory distress syndrome. *Am Rev Respir Dis* 147: 218–233, 1993.
23. Malarkkan N, Snook NJ, and Lumb AB. New aspects of ventilation in acute lung injury. *Anaesthesia* 58: 647–667, 2003.
24. Mantell LL, Shaffer TH, Horowitz S, Wolfson MR, Cox C, Khullar P, Zakeri Z, Lin L, Kazzaz JA, Palaia T, Scott W, and Davis JM. Distinct patterns of apoptosis in the lung during liquid ventilation compared with gas ventilation. *Am J Physiol Lung Cell Mol Physiol* 283: L31–L41, 2002.
25. Mates EA, Jackson JC, Hildebrandt J, Truog WE, Standaert TA, and Hlastala MP. Respiratory gas exchange and inert gas retention during partial liquid ventilation. *Adv Exper Med Biol* 361: 427–435, 1994.
26. Meinhardt JP, Ashton BA, Annich GM, Quintel M, and Hirschl RB. The dependency of expiratory airway collapse on pump system and flow rate in liquid ventilated rabbits. *Eur J Med Res* 8: 212–220, 2003.
27. Merritt TA, Kheiter A, and Cochrane CG. Positive end-expiratory pressure during KL4 surfactant instillation enhances intrapulmonary distribution in a simian model of respiratory distress syndrome. *Pediatr Res* 38: 211–217, 1995.
29. Nieman GF, Cigada M, Paskanik AM, Delpozzo J, Clark WR, Camporesi EM, and Hakim TS. Comparison of high-frequency jet to conventional mechanical ventilation in the treatment of severe smoke-inhalation injury. *Burns* 20: 157–162, 1994.
30. Paulson TE, Spear RM, Silva PD, and Petersen BM. High-frequency pressure-control ventilation with high positive end-expiratory pressure in children with acute respiratory distress syndrome. *J Pediatr* 129: 566–573, 1996.
31. Ruppert D. What is kurtosis: an influence function-approach. *Am Stat* 41: 1–5, 1987.
32. Segerer H, Scheid A, Wagner MH, Lekka M, and Obladen M. Rapid tracheal infusion of surfactant versus bolus instillation in rabbits: effects on oxygenation, blood pressure and surfactant distribution. *Biol Neonate* 69: 119–127, 1996.
33. Shaffer TH. A brief review: liquid ventilation. *Undersea Biomed Res* 14: 169–179, 1987.
34. Shaffer TH, Wolfson MR, and Clark L Jr. State of the art review: liquid ventilation. *Pediatr Pulmonol* 14: 102–109, 1992.
35. Shaffer TH, Wolfson MR, and Clark LC Jr. Liquid ventilation. *Ped Pulm* 14: 102–109, 1992.
36. Shaffer TH, Wolfson MR, Greenspan JS, Rubenstein SD, and Stern RG. Perfluorochemical liquid as a respiratory medium. *Artif Cells Blood Substit Immobil Biotechnol* 22: 315–326, 1994.
37. Skoog DA and West DM. *Analytical Chemistry*. New York: Holt, Rinehart, and Winston, 1965.
38. Ueda T, Ikegami M, Rider ED, and Jobe AH. Distribution of surfactant and ventilation in surfactant-treated preterm lambs. *J Appl Physiol* 76: 45–55, 1994.
39. Wolfson MR, Greenspan JS, Deoras KS, Rubenstein SD, and Shaffer TH. Comparison of gas and liquid ventilation: clinical, physiological, and histological correlates. *J Appl Physiol* 72: 1024–1031, 1992.